Virology 535 (2019) 210–217

Contents lists available at ScienceDirect

Virology

journal homepage: www.elsevier.com/locate/virology

Implication of whitefly vesicle associated membrane protein-associated protein B in the transmission of *Tomato yellow leaf curl virus*

Jing Zhao, Yao Chi, Xin-Jia Zhang, Xiao-Wei Wang, Shu-Sheng Liu*

Ministry of Agriculture Key Laboratory of Molecular Biology of Crop Pathogens and Insects, Institute of Insect Sciences, Zhejiang University, Hangzhou, 310058, PR China

ARTICLE INFO

Keywords:
TYLCV
Whitefly
VAPB
Transmission

ABSTRACT

Tomato yellow leaf curl virus (TYLCV) poses serious threat to tomato production worldwide, and the vector, *Bemisia tabaci*, plays a key role in the transmission of this virus. However, the molecular mechanisms underlying the transmission remain poorly understood. In this study, firstly, we identified the whitefly proteins that presumably interact with TYLCV coat protein (CP) using split-ubiquitin yeast two-hybrid system. Next, we conducted GST pull-down and immunofluorescence to examine the potential interaction between TYLCV CP and one of the proteins identified, namely vesicle associated membrane protein-associated protein B (VAPB), an protein abundantly expressed in whitefly midgut. Further experiments demonstrated that VAPB was significantly upregulated upon virus acquisition, and silencing VAPB led to a significant increase of relative virus quantity in whitefly haemolymph and salivary glands, as well as an increase of TYLCV transmission efficiency. These findings indicate an important role of VAPB in the transmission of TYLCV by whiteflies.

1. Introduction

Plant viral diseases represent a major constraint to the production of many crops, and one of the most destructive viral diseases is tomato yellow leaf curl disease (Moriones and Navas-Castillo, 2000; Scholthof et al., 2011; Navas-Castillo et al., 2011). As a notorious viral disease in tomato production worldwide, tomato yellow leaf curl disease can be caused by many viruses in the genus *Begomovirus*, among which tomato yellow leaf curl virus (TYLCV) has been found to be most widely distributed (Cohen and Antignus, 1994; Diaz-pendon et al., 2010; Navas-Castillo et al., 2011). TYLCV is transmitted by whiteflies of the *Bemisia tabaci* cryptic species complex in a persistent circulative manner (Hogenhout et al., 2008; Ghanim et al., 2001). Once acquired orally by whitefly, TYLCV follows a sequential path of stylet-midgut-haemolymph-salivary gland, and in this journey inside whitefly, virus has to cross two major physiological barriers, namely midgut and salivary gland, to be transmitted successfully by vector (Ghanim et al., 2001; Brown and Czosnek, 2002; Hogenhout et al., 2008; Rosen et al., 2015; Czosnek et al., 2017). As midgut is the first barrier virus encounters, advances in understanding the process of virus transport across the midgut are instrumental in deciphering the nature of TYLCV-whitefly interactions at cellular and molecular levels. However, the process of TYLCV transport across the midgut cells remain hitherto understudied, and only a limited number of cellular factors has been identified, viz. vesicle trafficking systems, clathrin-mediated endocytosis and early endosome network (Uchibori et al., 2013; Pan et al., 2017; Czosnek et al., 2017; Xia et al., 2018).

For insect-borne viruses, productive transmission entails specific interactions of viral proteins with cellular proteins of the vector to facilitate virus transport in and out of insect tissues (Gray and Banerjee, 1999). For begomoviruses including TYLCV, the coat protein (CP) is the only structural protein known to be involved in the virus transmission by whitefly (Harrison et al., 2002; Czosnek et al., 2017). CP is located on the surface of virions, and in the virus circulative journey inside whitefly, CP is in contact with various tissues and proteins of whitefly (Ghanim et al., 2001; Czosnek et al., 2017). For whitefly, a few cellular proteins have been reported to potentially interact with begomovirus CP, e.g., a member of the small heat-shock protein BtHSP16, GroEL produced by the endosymbiont *Hamiltonella* or *Arsenophonus*, heat shock protein 70, a midgut protein, cyclophilin B, a peptidoglycan recognition protein BtPGR, collagen and a thioredoxin-like protein (Ohnesorge and Bejarano, 2010; Gottlieb et al., 2010; Rana et al., 2012, 2015, 2019; Götz et al., 2012; Kanakala and Ghanim, 2016; Wang et al., 2016; Saurav et al., 2019). While these proteins have been shown to be associated with begomovirus CP, none of them has been ascribed to specific cellular processes such as vesicle trafficking. Since the role of vesicle trafficking systems of whitefly in virus transport has been appreciated, it is urgent to learn about the underlying molecular

* Corresponding author.
E-mail address: shshliu@zju.edu.cn (S.-S. Liu).

https://doi.org/10.1016/j.virol.2019.07.007
Received 10 May 2019; Received in revised form 5 July 2019; Accepted 5 July 2019
Available online 11 July 2019

mechanisms such as the protein-protein interactions involved.

In this study, firstly, using split-ubiquitin yeast-two hybrid (Y2H) assay, we identified a number of whitefly proteins that presumably interact with TYLCV CP, including one vesicle-associated protein named vesicle associated membrane protein-associated protein B (VAPB), which was expressed dominantly in whitefly midgut. Secondly, we examined the putative interaction of VAPB with TYLCV CP *in vitro* and *in vivo*. Next, we characterized the transcription and expression of whitefly VAPB upon virus acquisition. Finally, with the aid of dsRNA micro-injection, we experimentally investigated the role of VAPB in virus acquisition and transmission by whiteflies. Our findings provide new insights into the nature of TYLCV-whitefly interactions.

2. Materials and methods

2.1. Insect, virus and plants

A population of MEAM1 whiteflies (mt*COI* GenBank Accession code: GQ332577) was collected from the field and then maintained on cotton plants (*Gossypium hirsutum* L. cv. Zhemian 1793) in insect proof cages in the laboratory. For virus, infectious clones of TYLCV isolate SH2 (GenBank accession code: AM282874) were provided by Professor Xue-Ping Zhou (Institute of Biotechnology, Zhejiang University). Infectious clone was agro-inoculated into tomato plants (*Solanum lycopersicom* L. cv. Hezuo903) when they reached the stage of 3–4 true leaves, and then the virus-inoculated plants were further cultured to the stage of 7–8 true leaves to obtain TYLCV-infected plants for experiments. Un-infected tomato plants used as control were also cultivated to the stage of 7–8 true leaves for further experiments. All insect rearing and ecological experiments were conducted in climate chambers at 26 ± 1 °C, 60% relative humidity and a photoperiod of 14 h light/10 h darkness.

2.2. Split-ubiquitin Y2H system

We used the Y2H system based on split-ubiquitin (Dualsystems BioTech, Switzerland) to screen for proteins in whitefly that potentially interact with TYLCV CP. Fig. 1 illustrates the experimental procedure. Firstly, the full-length of TYLCV CP gene was inserted into the bait plasmid pDHB1, and the whitefly cDNA library was constructed and ligated into the prey plasmid pPR3-N. Then, the bait plasmid pDHB1-TYLCV CP was transformed into NMY51 yeast strain, and the transformation was then verified using synthetic defined minimal medium lacking leucine (S.D./-Leu). The expression of TYLCV CP in the yeast was confirmed by western blot with *anti*-TYLCV CP mouse monoclonal antibody (mAb) (provided by Professor Jian-Xiang Wu, Institute of Biotechnology, Zhejiang University). Next, the whitefly cDNA library was transformed into the NMY51 yeast strain in which the expression of TYLCV CP was verified. The growth of yeast strain on double dropout medium (DDO: S.D./-Leu/-Trp) and triple dropout medium (TDO: S.D./-His/-Leu/-Trp) with 1 mm 3-aminotriazole (3-AT) was observed. Positive clones were picked out from the TDO with 1 mm 3-AT, and then verified on quadruple dropout medium (QDO: S.D./Ade/-His/-Leu/-Trp). Afterwards the detection of beta-galactosidase activity was conducted using the yeast beta-Gal assay kit (Thermo Scientific, USA). Finally, plasmids from the positive clones were extracted and transformed into *E. coli* strain DH5α, and then sequenced to identify candidate proteins that potentially interact with TYLCV CP in whitefly. The sequences obtained were annotated using BLAST (http://blast.st-va.ncbi.nlm.nih.gov/Blast.cgi). For verification of the interaction, the full length of *VAPB* was amplified and cloned into pPR3-N, and then verification of interaction was conducted with the methods described above. Table S1 presents primers used here.

2.3. Analysis of VAPB transcription level

For analysis of *VAPB* transcription level in whitefly midgut, 100 midguts were obtained via dissecting 100 female whitefly adults and collected as the test material of one replicate, and three replicates were analysed. For analysis of *VAPB* transcription level in whitefly carcass, midguts of 30 females were removed and the remains, i.e., carcass, were collected as the test material of one replicate, and three replicates were analysed. For analysis of *VAPB* transcription level in whitefly whole body, 30 adults were killed and collected as the test material of one replicate, and three replicates were analyzed. Total RNA was isolated using TRIzol (Invitrogen, USA). Reverse transcription was

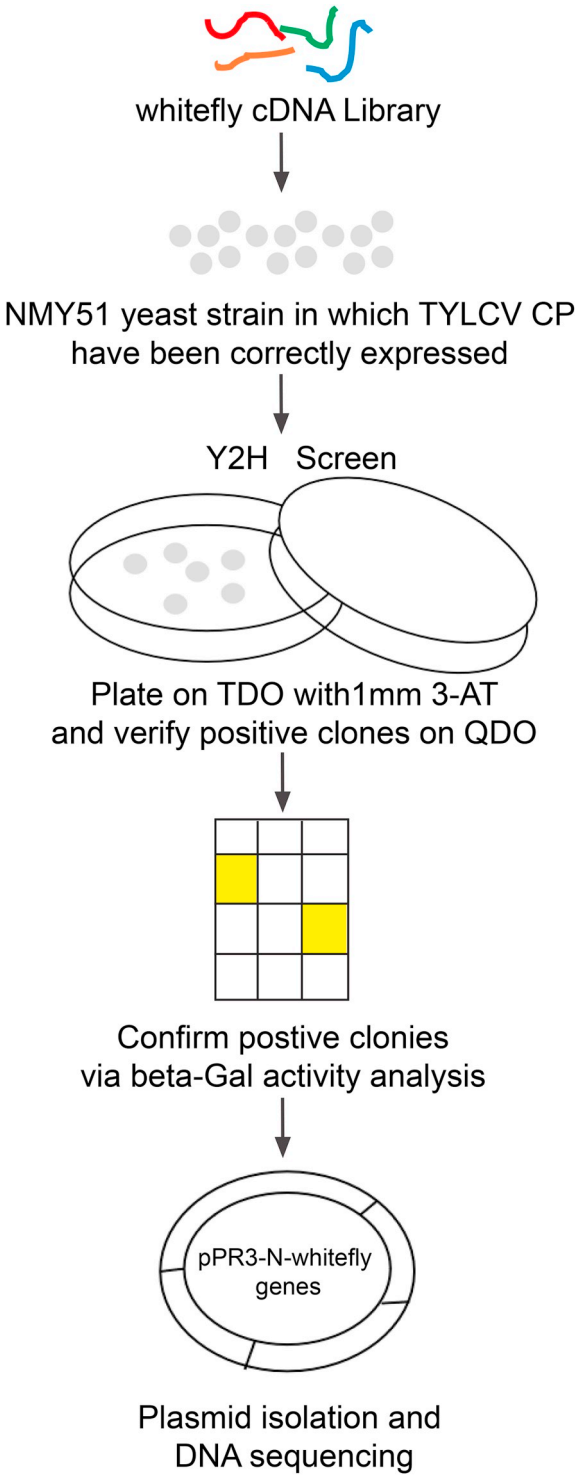

Fig. 1. Schematic diagram of workflow for the split-ubiquitin Y2H assay system.

conducted using PrimeScript™ RT reagent kit with gDNA eraser (TaKaRa, Japan) following the manufacturer's manual. qPCR was performed on CFX connect Real-Time PCR system (Bio-Rad, USA) using the TB Green™ Premix Ex Taq™ II (TaKaRa, Japan). Primers used are listed in Table S1.

2.4. GST pull-down assay

The full length of TYLCV CP gene was cloned into pGEX-6p-1 for fusion with GST tag, and the fragments of *VAPB* with transmembrane region eliminated (VAPBΔTM) and the SCS2 domain of *VAPB* was amplified and cloned into pMAL-c5x for fusion with MBP tag respectively. Primers used here are listed in Table S1. Recombinant protein was expressed in *E. coli* strain Rosetta and purified. The fusion protein GST-TYLCV CP and GST (control) was then bound to glutathione agarose beads (GE Healthcare, USA) for 2 h at 4 °C and then washed. MBP-VAPBΔTM, MBP-SCS2 and MBP (control) were purified and desalinated, and then they were incubated with the glutathione agarose beads bounded with GST-TYLCV CP or GST for 4 h at 4 °C, respectively. Next, the mixture was washed by 1 × PBS for 3–5 times, and then the beads-bound proteins were eluted by boiling in PAGE buffer (FDbio, China) for 10 min. Finally, the proteins were separated by SDS/PAGE gel electrophoresis and detected by *anti*-MBP rabbit polyclonal antibody (pAb) (Abcam, UK) and *anti*-GST mouse mAb (Cell Signaling Technology, USA) respectively.

2.5. Immunofluorescence detections of TYLCV and VAPB in whitefly midguts

Immunofluorescence detections of proteins were performed as follows: briefly, midguts were obtained by dissection of female whiteflies and fixed for 2 h with 4% paraformaldehyde in 1 × PBS. After washing 3 times in 1 × PBS, midguts were blocked and permeabilized using 0.4% Triton X-100 in 3% BSA for 2 h, followed by incubation with primary antibodies (overnight at 4 °C). The next day, after washing 3 times in 1 × PBS, midguts were incubated with secondary antibodies for 1–2 h at room temperature, and then washed 3 times in 1 × PBS. Finally, midguts were mounted in fluoroshield mounting medium with DAPI (Abcam, USA) and examined under LSM 780 (ZEISS, Germany). Detection of whitefly VAPB was conducted with *anti*-VAPB mouse mAb (Abcam, UK) and Alexa Fluor 549 conjugated goat anti-mouse secondary antibody (Earthox, China), and detection of TYLCV CP was conducted with *anti*-TYLCV CP rabbit pAb (provided by Professor Jian-Xiang Wu, Institute of Biotechnology, Zhejiang University) and goat anti-rabbit secondary antibody conjugated with Alexa Fluor 647 (Invitrogen, USA) for co-localization analysis, or *anti*-TYLCV CP mouse mAb and goat anti-mouse secondary antibody conjugated with Alexa Fluor 549 (Earthox, China) for virus quantity analysis. The fluorescence intensities and plot profile analysis of fluorescent gray value were generated by ImageJ software.

2.6. Synthesis of dsRNA and micro-injection

DsRNA synthesis was conducted using T7 high yield transcription kit (Vazyme, China) following the manufacturer's instruction. Briefly, template with T7 promoters at both ends was amplified using specific primers for *VAPB* and *GFP* (control), and the purified PCR products were used in the synthesis. Primers used for the synthesis of DNA templates are listed in Table S1. DsRNA was purified and the quality was determined by agarose gel electrophoresis. Micro-injection was performed using FemtoJet (Eppendorf, USA), and on average 6 nL of purified dsRNA (2 μg/μL) was injected into the thorax of each of the adult whiteflies. Following micro-injection, whiteflies were allowed to recover via feeding on cotton plants for two days, and then for virus acquisition. To assess the levels of *VAPB* transcription and expression in control and treated whiteflies, qPCR and Western blot analysis were conducted as described in 2.3 and 2.9. Immunofluorescence described in 2.5 was performed to determine the VAPB level in the midgut of silenced whiteflies.

Table 1
BLAST search of NCBI database for candidate binding partners of TYLCV CP in whitefly.

Accession	Protein Name
XP_018905345.1	Vesicle-associated membrane protein-associated protein B-like
XP_018897111.1	PDZ and LIM domain protein Zasp-like isoform X5
XP_018900655.1	Zinc finger with UFM1-specific peptidase domain protein-like
XP_018902946.1	Cytochrome *b*5-like isoform X2
XP_018899115.1	Charged multivesicular body protein 7
XP_018905767.1	Protein D3-like
XP_018917964.1	Probable cytochrome P450 6a13 isoform X1

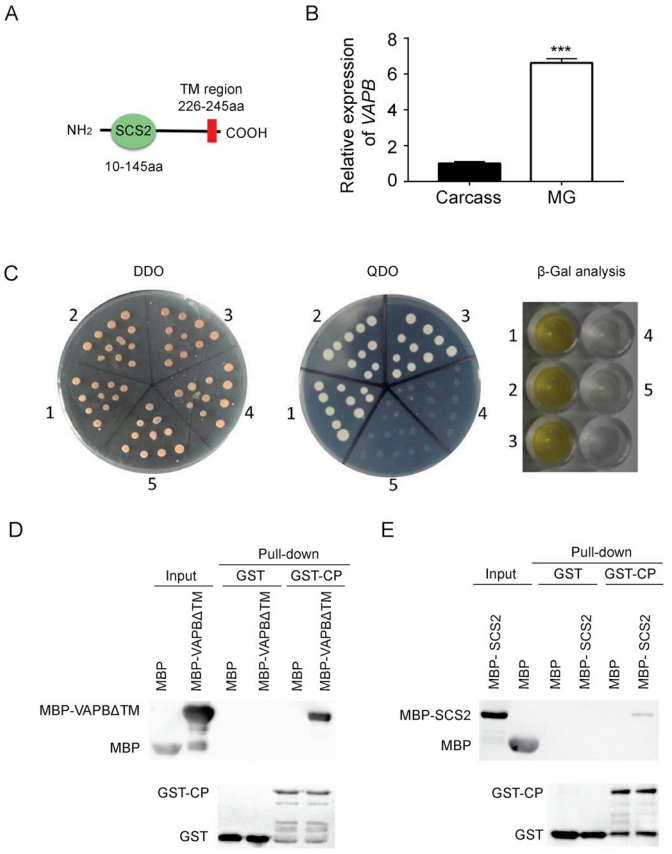

Fig. 2. Verification of interaction between VAPB and TYLCV CP *in vitro*. (A) Schematic presentation of VAPB structure. (B) *VAPB* transcription levels in whitefly midgut and carcass. Female whitefly adults that had emerged within one week were used for dissection and analysis. Data are presented as mean ± SEM, n = 3 (Student's *t*-test, ***$P < 0.001$). (C) Split-ubiquitin yeast two hybrid assay. 1: pDHB1-largeT + pOst-Δp53(positive control), 2: pDHB1-CV-CP + pOst-NubI (positive control), 3: pDHB1-CV-CP + pPR3-N-VAPB, 4 pDHB1-largeT + pPR3-N (negative control), 5: pDHB1-CV-CP + pPR3-N (negative control). Yeasts were plated on DDO and QDO, and clones were picked out for beta-Gal assay. (D) The interaction between GST-TYLCV CP and MBP-VAPBΔTM via GST pull-down analysis. (E) The interaction between GST-TYLCV CP and MBP-SCS2 via GST pull-down analysis.

2.7. Virus acquisition and transmission by whiteflies

For VAPB level analysis following virus infection, whitefly adults that had emerged within one week were collected and caged on the same branch of a TYLCV-infected tomato plant for 0 h, 24 h, 48 h or

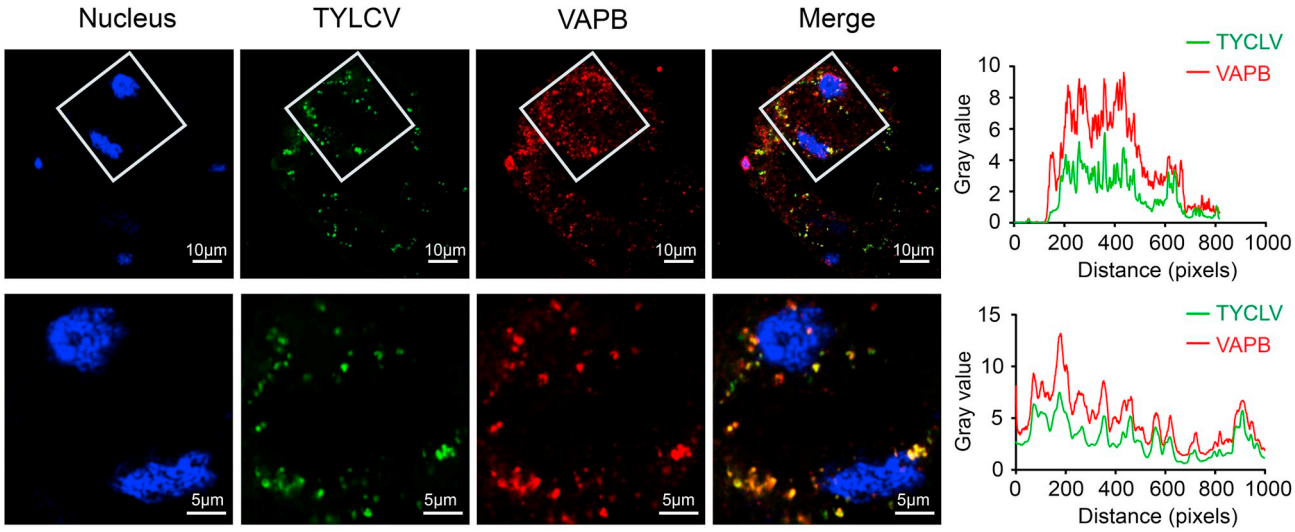

Fig. 3. Co-localization of TYLCV CP (green) and VAPB (red) in whitefly midgut cells. Female whiteflies that had fed on TYLCV-infected tomato plants for 48 h were collected, and their midguts were dissected for immunofluorescence detection of VAPB and TYLCV CP. Whitefly VAPB was detected with *anti*-VAPB mouse mAb and Alexa Fluor 549 conjugated secondary antibody (red), and TYLCV CP was detected with *anti*-TYLCV CP rabbit pAb and secondary antibody conjugated with Alexa Fluor 647 (green). Nucleus was stained with DAPI (Alexa Fluor 405, blue).

96 h, respectively, to acquire virus, and an un-infected tomato plant was used as control. Following dsRNA micro-injection and recovery, control and treated whiteflies were respectively caged with two symmetrical leaves of a TYLCV-infected tomato plant for 24 h. For virus transmission, whiteflies that had acquired virus for 24 h were collected and allowed to feed on a true leaf of un-infected tomato seedlings (3–4 true leaf stage) for 48 h. Whiteflies were then removed, and plants were sprayed with imidacloprid (50 mg/L) to kill the eggs. Thirty days later, TYLCV infection in plants was examined by diagnostic PCR. For each treatment, ten plants were used. Primers used for TYLCV detection are listed in Table S1.

2.8. Analysis of quantity of virus in whitefly whole body and tissues

For analysis of quantity of virus in whitefly whole body, 10 females were collected as the material of one replicate, and three replicates were conducted. For midgut, 10 midguts of females were obtained by dissection and collected as the material of one replicate and three replicates were analyzed. For haemolymph, the abdomen of female whiteflies were punctured individually in 10 μL 1 × PBS, and then the midgut was removed, 8 μL of the mixture of haemolymph and PBS was collected and subjected to DNA extraction using lysis buffer. For salivary glands, a pair of salivary glands from individual female whiteflies was dissected and collected. The number of samples analyzed for haemolymph and salivary glands were 31 and 26–29 respectively. The details of DNA extraction by lysis buffer were the same as reported previously (Pan et al., 2017). qPCR was conducted as described in section 2.3. Primers used are listed in Table S1.

2.9. Western blot

To analyze the quantity of VAPB and TYLCV CP at protein level, 100 whiteflies were collected as a sample. Total protein was extracted by RIPA (Beyotime, China) and subjected to Western blot analysis using *anti*-VAPB mouse mAb, *anti*-TYLCV CP mouse mAb and *anti*-β-actin mouse mAb (Earthox, China) depending on design of the experiment. The concentration of total protein was monitored using BCA protein assay (Thermo Scientific, USA), and equal amount of total protein was loaded for each of the samples.

2.10. Statistical analysis

Prior to analysis, all raw time data were calculated using the $2^{-\triangle Ct}$ method as normalized to whitefly *β-actin*. Comparison of the quantity of virus in whitefly whole body and tissues, gene transcription levels of *VAPB* and fluorescence intensities of CP or VAPB were performed using Student's independent *t*-test. Difference was considered significant when $P < 0.05$ ($^{*}P < 0.05$, $^{**}P < 0.01$, $^{***}P < 0.001$). Nonparametric Chi-square test was used to compare the transmission efficiency of TYLCV by whiteflies. All the statistical analyses were performed using SPSS 20.0 (SPSS Inc., USA).

3. Results

3.1. Identification of whitefly proteins that potentially interact with TYLCV CP

Fig. 1 shows the workflow of split-ubiquitin yeast two hybrid (Y2H) system used to identify proteins in whitefly that potentially interact with TYLCV CP. We constructed a whitefly cDNA library with three open read frames, the capacity of which was greater than 3.0×10^6 cfu. The practical amplification base of this library was more than 1.5 million cfu and the inserted fragments of whitefly genes were 500–3000 bp in length, indicating the fine quality of the cDNA library we constructed (Fig. S1A). The expression of bait plasmid pDHB1-TYLCV CP in yeast was verified by Western blot analysis (Fig. S1B). Co-transformation of the pDHB1-TYLCV CP and the prey plasmid pOst1-NubI (positive control) in yeast resulted in growth of yeast on all selective media, whereas the co-transformation of pDHB1-TYLCV CP and prey plasmid pPR3-N (negative control) did not grow on the TDO and QDO (Fig. S1C), suggesting that the bait plasmid pDHB1-TYLCV CP was functionally well expressed in the split-ubiquitin Y2H system. The transformation efficiency in our assay was 1.584×10^5. Totally, after screening of whitefly cDNA library using this Y2H system, 19 positive clones were isolated and 7 candidate whitefly proteins were identified (Table 1).

3.2. Verification of the interaction between VAPB and TYLCV CP in vitro

Previous studies show that viruses in the whitefly midgut cells were enclosed in vesicles (Uchibori et al., 2013; Xia et al., 2018). In the

candidate proteins identified, we found a vesicle-associated protein VAPB (XP_018905345.1) with a SCS2 domain (10-145aa) and a transmembrane region (226-245aa) (Fig. 2A), which was subjected to further analysis due to its putative role in intracellular vesicle trafficking. According to the MEAM1 whitefly midgut transcriptome database (https://www.ncbi.nlm.nih.gov/bioproject/PRJNA407873/), *VAPB* is well expressed in whitefly midgut. To further examine the *VAPB* level in whitefly midgut, qPCR analysis was conducted. As shown in Fig. 2B, when compared with whitefly carcass, whitefly midgut has a much higher transcription of *VAPB*. Then, we examined the interaction between VAPB and TYLCV CP in Y2H and found a strong association between them (Fig. 2C). Next, we performed GST-Pull down assay to further verify the interaction between VAPB and TYLCV CP. To increase the solubility of protein when expressed in prokaryotic cells, we eliminated the transmembrane region of VAPB (VAPBΔTM), and then the MBP-VAPBΔTM fusion protein or MBP-SCS2 domain were expressed in *Escherichia coli* strain Rosetta and purified. GST pull-down analysis showed that the interaction between TYLCV CP and VAPB was independent of the transmembrane region (Fig. 2D and E).

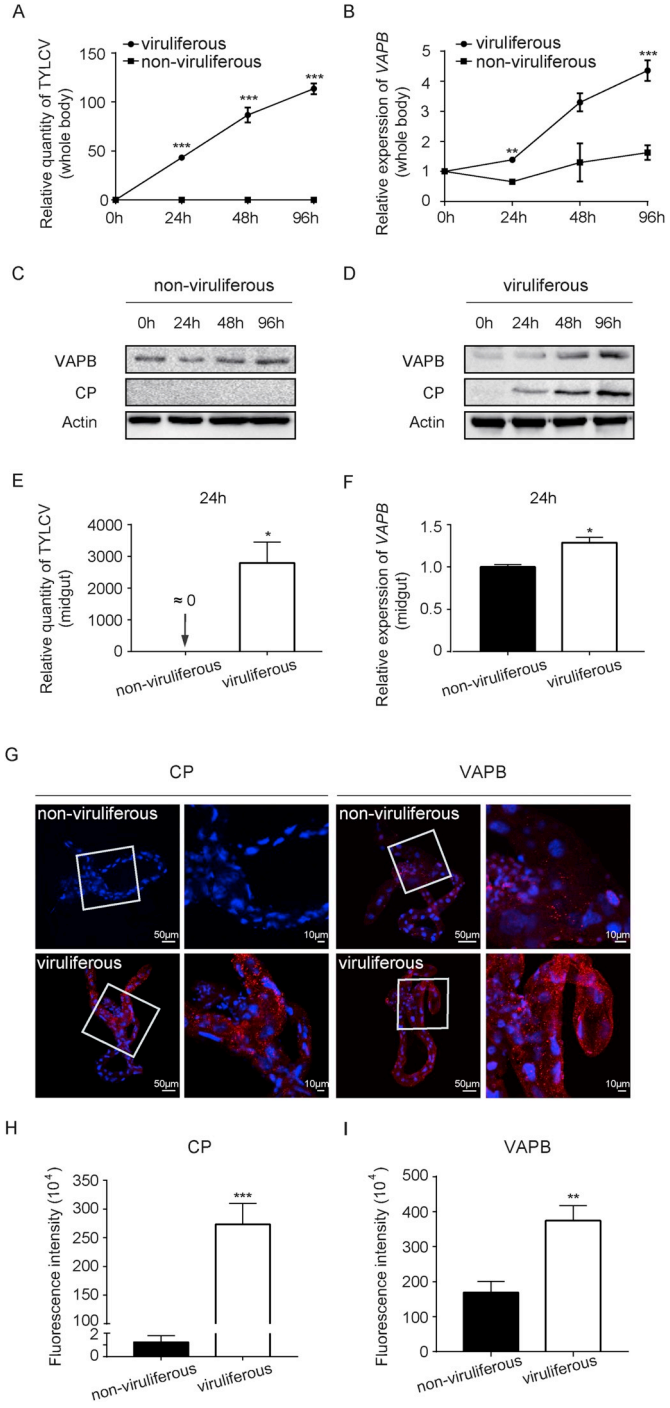

Fig. 4. Effect of TYLCV infections on the transcription and expression of *VAPB*. Analyses in A-D were conducted with whiteflies that fed consecutively on TYLCV-infected and un-infected plants for 0 h, 24 h, 48 h and 96 h respectively. Analyses in E-I were conducted with whiteflies that fed on TYLCV-infected and un-infected plants for 24 h. (A) Quantity of virus in whitefly whole body. (B) Level of *VAPB* transcription in whitefly whole body. (C–D) Western blot analysis of VAPB expression and TYLCV CP in the whole body of un-infected whitefly (C) and TYLCV-infected whitefly (D). β-Actin was used as control. (E) Quantity of virus in whitefly midgut. (F) Level of *VAPB* transcriptions in whitefly midgut. (G) Immunofluorescence detection of VAPB and TYLCV levels in whitefly midgut. Whitefly VAPB and TYLCV CP were detected with their corresponding mouse mAb, respectively and Alexa Fluor 549 conjugated secondary antibody (red). Nucleus was stained with DAPI (Alexa Fluor 405, blue). The midguts shown here were selected from representative images in Fig. S2. (H–I) Fluorescence intensities of TYLCV CP (H) and VAPB (I) in whitefly midgut. Representative images that were used to generate the data here are provided in Fig. S2. For A-B and E-F, three replicates were analyzed for each combination of whitefly status and time interval, and data are presented as mean ± SEM, n = 3; For H–I, six midguts were used for analysis, data are presented as mean ± SEM, n = 6 (Student's *t*-test, $^{*}P < 0.05$, $^{**}P < 0.01$, $^{***}P < 0.001$).

3.3. Co-localization of VAPB and TYLCV CP

The Y2H and GST pull-down analysis indicates interaction between VAPB and TYLCV CP *in vitro*, and to further investigate whether TYLCV CP had a co-localization with VAPB *in vivo*, immunofluorescence detection of VAPB and TYLCV CP in whitefly midgut was performed. VAPB and TYLCV CP were labeled with Alexa Fluor 549 (red) and Alexa Fluor 647 (green) respectively, and the result showed a clear co-localization of VAPB and TYLCV CP within whitefly midgut cells (Fig. 3), suggesting that VAPB and TYLCV CP may interact *in vivo*.

3.4. Transcription and expression of whitefly VAPB upon TYLCV acquisition

To explore the patterns of *VAPB* transcription and expression in whitefly upon virus acquisition, whiteflies were allowed to feed on TYLCV-infected tomato for four different virus acquisition access periods (AAP), then, the quantity of virus and level of *VAPB* transcriptions and expressions in whitefly whole body were analyzed. Real-time PCR data showed that the relative virus quantity in whiteflies increased with the increase of acquisition access period (Fig. 4A). At the same time, *VAPB* transcription in viruliferous whiteflies also increased with the increase of acquisition access period and was significantly higher than control at two time points (Fig. 4B). Analysis of protein level of VAPB showed a similar pattern (Fig. 4C and D). Furthermore, to explore whether or not the level of VAPB in whitefly midgut could be regulated by virus infection, the midgut of whitefly females that have consecutively acquired virus for 24 h were dissected and subjected to analysis of *VAPB* transcription. As shown in Fig. 4E and F, following virus acquisition, *VAPB* transcription in the midguts of viruliferous whitefly showed a significant up-regulation. Further, fluorescent signals of VAPB in the midguts of TYLCV-infected whiteflies were significantly stronger than those in the midguts of non-viruliferous whiteflies (Fig. 4G–I).

3.5. Effect of silencing VAPB on virus acquisition and transmission by whitefly

We used RNA interference triggered by dsRNA to explore the role of

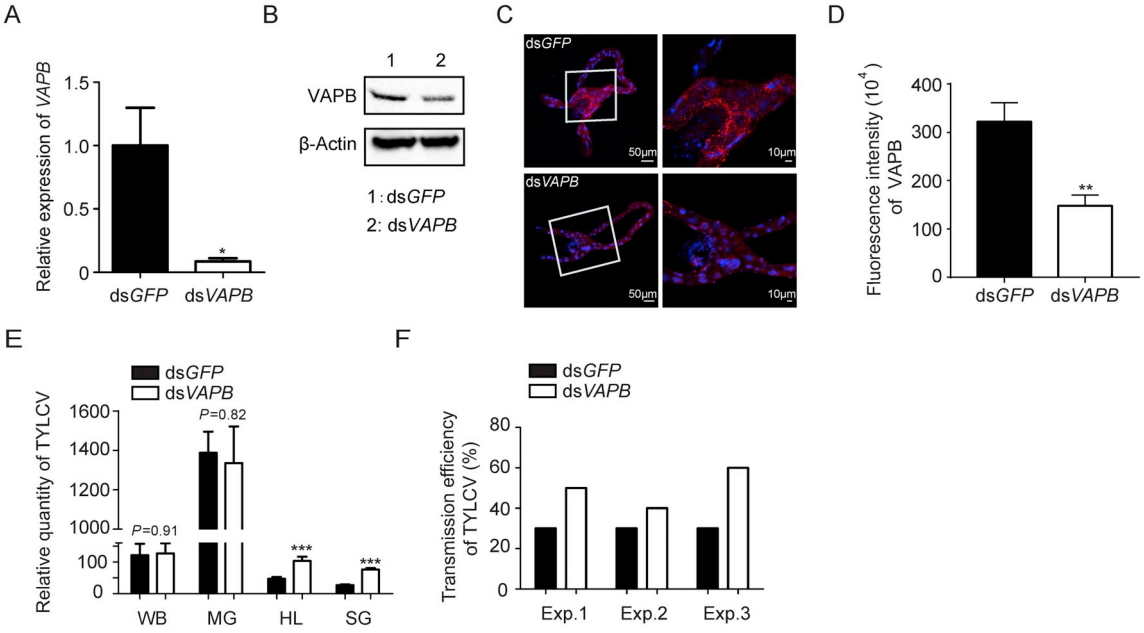

Fig. 5. Level of *VAPB*, quantity of virus in whitefly and efficiency of TYLCV transmission by whiteflies receiving dsRNA treatment. (A) The relative gene transcription level of *VAPB* in whitefly following dsRNA treatment. (B) Expression level of *VAPB* following dsRNA treatment. β-Actin was used as control. (C) Detection of VAPB in the midgut of ds*GFP* or ds*VAPB*-treated whiteflies. VAPB was detected with *anti*-VAPB mouse mAb and Alexa Fluor 549 conjugated goat anti-mouse secondary antibody (red), nucleus was stained with DAPI (Alexa Fluor 405, blue). The midguts shown here were selected from representative images in Figure S3 (D) Fluorescence intensities of VAPB in the midgut of control and treated whitefly. Representative images that were used to generate the data here are provided in Figure S3. (E) Relative quantity of virus in whole body (WB), midgut (MG), haemolymph (HL) and salivary gland (SG) of whitefly. The virus levels presented here were calculated using $2^{-\triangle Ct}$ as normalized to whitefly β-actin. (F) Efficiency of virus transmission by whiteflies that were given 48 h for TYLCV acquisition after ds*VAPB* treatment. Three replicates were conducted for each of the treatments presented in (A), WB, MG in (E), six midguts were analyzed for D, and 26–31 samples were analyzed for HL and SG in (E). Three replicates with each containing 10 test plants were conducted for F (Student's *t*-test, $*P < 0.05$, $**P < 0.01$, $***P < 0.001$ for A and D-E; Nonparametric Chi-square test for F, $P = 0.325$, 0.500 and 0.185 for replicate 1, 2, 3 respectively).

whitefly VAPB in virus acquisition and transmission. The silencing efficiency of *VAPB* was about 91%, showing the high validity of the dsRNA micro-injection (Fig. 5A). Western blot was conducted to examine the decreased expression of VAPB in silenced whiteflies (Fig. 5B). The levels of VAPB in control and treated whitefly midguts were analyzed by immunofluorescence, also suggesting a decreased VAPB level in whitefly midgut following dsRNA micro-injection (Fig. 5C and D). Interestingly, silencing of *VAPB* did not significant change the quantity of virus in the whole body and midgut of whitefly, but resulted in significant increases of virus titer in the haemolymph and salivary glands (Fig. 5E). Silencing *VAPB* also increased the efficiency of TYLCV transmission by whiteflies in each of the three independent experiments (Fig. 5F).

4. Discussion

In whitefly, vesicle trafficking system in midgut cells has been shown to play an important role in the transport of TYLCV across the midgut basal membrane to haemolymph (Uchibori et al., 2013; Xia et al., 2018). However, during virus intracellular vesicle trafficking, whitefly proteins associated with this process remain largely unknown. Herein, we used split-ubiquitin Y2H system to investigate the putative binding partners of TYLCV CP in whitefly. A vesicle associated membrane protein-associated protein (VAP), namely VAPB, was identified and subjected to further study. Consistent with the MEAM1 whitefly midgut transcriptome database (https://www.ncbi.nlm.nih.gov/bioproject/PRJNA407873/), our data show that VAPB is abundant in whitefly midgut. GST-Pull down verified the interaction between VAPB and TYLCV CP *in vitro*, and immunofluorescence assay demonstrated their co-localizations *in vivo*. The level of VAPB following virus acquisition was significantly up-regulated, while silencing *VAPB* led to increase of the relative virus quantity in whitefly haemolymph and salivary glands as well as virus transmission efficiency.

As regulators of soluble N-ethylmaleimide-sensitive fusion protein attachment protein receptors, VAP porteins are involved in the intracellular vesicle trafficking (Weir et al., 1998). Over-expression of protein VAP-A prevented the export of insulin-dependent glucose transporter 4 to the cell surface in L6 myoblasts (Nishimura et al., 1999; Foster et al., 2000). The N-terminal protein p48 of Norwalk virus forms a complex with VAP-A, and this complex disrupts the trafficking of vesicular stomatitis virus G glycoprotein to the cell surface (Ettayebi and Hardy, 2003). Weir et al. (1998), probably for the first time, demonstrated the involvement of VAP in mammalian vesicle fusion during exocytosis. Skehel et al. (2000) described a role of VAP in the function of mammalian neurons. A mutation in VAPB causes familial amyotrophic lateral sclerosis type 8 (Nishimura et al., 1999), and the involvement of human VAPB in *Hepatitis C virus* replication was reported by Hamamoto et al. (2005).

In view of the general nature of VAP proteins described above and the virus transport path of stylet-midgut-haemolymph-salivary gland in whitefly (Ghanim et al., 2001; Brown and Czosnek, 2002; Hogenhout et al., 2008; Rosen et al., 2015; Czosnek et al., 2017), as well as higher virus levels in haemolymph and salivary gland of *VAPB* silenced whiteflies, we proposed that whitefly VAPB may function in the vesicle trafficking systems within whitefly midgut cells and prevents the virions from crossing the midgut escaping barrier in a yet unknown fashion. Based on this inference, it is understandable that whitefly exhibited better transmission capacity upon silencing VAPB. At the same time, in our experiments, it is interesting that though a significant increase of virus quantity in whitefly haemolymph and salivary glands, the quantity of virus in whitefly whole body and midgut was not significantly changed following whitefly *VAPB* being silenced. Considering the path of virus movement in the whitefly body, one may expect that an increase of virus in the haemolymph and salivary glands would

likely lead to a decrease of virus in the midgut as more virus would be expected to have crossed the midgut basal membrane. For this, we propose that in this case a relatively small decease of virus in the midgut would be unnoticeable because many more virions were present in vector midgut upon virus acquisition, and the relative virus quantity in the midgut was 10–30 times higher than that in the haemolymph and salivary glands (Fig. 5B). This distribution of the virus is in line with previous reports that after AAPs of 12–48 h, most viruses accumulate in the vector digestive tract (Czosnek et al., 2017). Together, our findings provide a new insight into the role of protein VAPB and may facilitate future research on whitefly proteins in virus transmission.

In addition to VAPB, six candidate proteins, presumably involved in various cellular processes, were identified in this study (Table 1). For example, the PDZ and LIM domains are modular protein interaction motifs associated with cytoskeleton and signal transduction (Schmeichel and Beckerle, 1994; Tsunoda et al., 1997; Sadler et al., 1992; Turner and Miller, 1994; Roof et al., 1997; Xia et al., 1997; Hagmann et al., 1998), and zinc finger with UFM1-specific peptidase domain protein is a deubiquitylating enzyme that may promote cellular responses to genotoxic stress (Haahr et al., 2018). Exploration of the roles of these proteins in the transmission of begomoviruses by whiteflies is likely to further advance our understanding of begomovirus-whitefly interactions. In addition, for Y2H screening, transformation efficiency should be in the range of 1.5×10^5 to 2.5×10^5 clones/μg DNA. In our assay, the transformation efficiency was 1.584×10^5, approaching the minimal of the range. In the future, attempts may be made to raise the transformation efficiency so that more whitefly proteins potentially interacting with virus CP can be discovered.

Acknowledgements

We thank Professor Myron Zalucki for his help in the preparation of this manuscript, Professor Jian-Xiang Wu, Institute of Biotechnology, Zhejiang University, for providing antibody against TYLCV CP, and our lab engineer Gen-Hong Yan for plant cultivation and maintenance of lab facilities. This study was financially supported by the National Natural Science Foundation of China (31672029) and a subcontract from the University of Greenwich under a project sponsored by the Bill & Melinda Gates Foundation (Investment ID OPP1149777).

Appendix A. Supplementary data

Supplementary data to this article can be found online at https://doi.org/10.1016/j.virol.2019.07.007.

References

Brown, J.K., Czosnek, H., 2002. Whitefly transmission of plant viruses. Adv. Bot. Res. 36, 65–76. https://doi.org/10.1016/S0065-2296(02)36059-2.

Cohen, S., Antignus, Y., 1994. Tomato yellow leaf curl virus (TYLCV), a whitefly-borne geminivirus of tomatoes. In: In: Harris, K.H. (Ed.), Advances in Disease Vector Research, vol. 10. Springer-Verlag, New York, pp. 259–288.

Czosnek, H., Hariton-Shalev, A., Sobol, I., Gorovits, R., Ghanim, M., 2017. The incredible journey of begomoviruses in their whitefly vector. Viruses 9, 273. https://doi.org/10.3390/v9100273.

Diaz-pendon, J.A., Canizares, M.C., Moriones, E., Bejarano, E.R., Czosnek, H., Navas-castillo, J., 2010. *Tomato yellow leaf curl viruses: ménage à trois* between the virus complex, the plant and the whitefly vector. Mol. Plant Pathol. 11, 441–450. https://doi.org/10.1111/j.1364-3703.2010.00618.x.

Ettayebi, K., Hardy, M.E., 2003. Norwalk virus nonstructural protein p48 forms a complex with the snare regulator VAP-A and prevents cell surface expression of vesicular stomatitis virus G protein. J. Virol. 77, 11790–11797. https://doi.org/10.1128/jvi.77.21.11790-11797.2003.

Foster, L.J., Lynnweir, M., Lim, D.Y., Liu, Z., Trimble, W.S., Klip, A., 2000. A functional role for vap-33 in insulin-stimulated GLUT4 traffic. Traffic 1, 512–521. https://doi.org/10.1034/j.1600-0854.2000.010609.x.

Ghanim, M., Morin, S., Czosnek, H., 2001. Rate of *Tomato yellow leaf curl virus* translocation in the circulative transmission pathway of its vector, the whitefly *Bemisia tabaci*. Phytopathology 91, 188–196. https://doi.org/10.1094/PHYTO.2001.91.2.188.

Gottlieb, Y., Zchorifein, E., Mozesdaube, N., Kontsedalov, S., Skaljac, M., Brumin, M., Sobol, I., Czosnek, H., Vavre, F., Fleury, F., Ghanim, F., 2010. The transmission efficiency of *Tomato yellow leaf curl virus* by the whitefly *Bemisia tabaci* is correlated with the presence of a specific symbiotic bacterium species. J. Virol. 84, 9310–9317. https://doi.org/10.1128/jvi.00423-10.

Götz, M., Popovski, S., Kollenberg, M., Gorovits, R., Brown, J.K., Cicero, J.M., Czosnek, H., Winter, S., Ghanim, M., 2012. Implication of *Bemisia tabaci* heat shock protein 70 in begomovirus-whitefly interactions. J. Virol. 86, 13241–13252. https://doi.org/10.1128/jvi.00880-12.

Gray, S.M., Banerjee, N., 1999. Mechanisms of arthropod transmission of plant and animal viruses. Microbiol. Mol. Biol. Rev. 63, 128–148.

Haahr, P., Borgermann, N., Guo, X., Typas, D., Achuthankutty, D., Hoffmann, S., Shearer, R., Sixma, T.K., Mailand, N., 2018. ZUFSP deubiquitylates K63-linked polyubiquitin chains to promote genome stability. Mol. Cell 70, 165–174. https://doi.org/10.1016/j.molcel.2018.02.024.

Hagmann, J., Grob, M., Welman, A., van Willigen, G., Burger, M.M., 1998. Recruitment of the LIM protein hic-5 to focal contacts of human platelets. J. Cell Sci. 111, 2181–2188.

Hamamoto, I., Nishimura, Y., Okamoto, T., Aizaki, H., Liu, M., Mori, Y., Abe, T., Sizilo, T., Lai, M.M.C., Miyamura, T., Moriishi, K., Matsuura, Y., 2005. Human VAP-B is involved in hepatitis C virus replication through interaction with NS5A and NS5B. J. Virol. 79, 13473–13482. https://doi.org/10.1128/JVI.79.21.13473-13482.2005.

Harrison, B.D., Swanson, M.M., Fargette, D., 2002. Begomovirus coat protein: serology, variation and functions. Physiol. Mol. Plant Pathol. 60, 257–271. https://doi.org/10.1006/pmpp.2002.0404.

Hogenhout, S.A., Ammar, E.D., Whitfield, A.E., Redinbaugh, M.G., 2008. Insect vector interactions with persistently transmitted viruses. Annu. Rev. Phytopathol. 46, 327–359. https://doi.org/10.1146/annurev.phyto.022508.092135.

Kanakala, S., Ghanim, M., 2016. Implication of the whitefly *Bemisia tabaci* cyclophilin B protein in the transmission of *Tomato yellow leaf curl virus*. Front. Plant Sci. 7, 1702. https://doi.org/10.3389/fpls.2016.01702.

Moriones, E., Navas-Castillo, J., 2000. *Tomato yellow leaf curl virus*, an emerging virus complex causing epidemics worldwide. Virus Res. 71, 123–134. https://doi.org/10.1016/S0168-1702(00)00193-3.

Navas-Castillo, J., Fiallo-Olivé, E., Sánchez-Campos, S., 2011. Emerging virus diseases transmitted by whiteflies. Annu. Rev. Phytopathol. 49, 219–248. https://doi.org/10.1146/annurev-phyto-072910-095235.

Nishimura, Y., Hayashi, M., Inada, H., Tanaka, T., 1999. Molecular cloning and characterization of mammalian homologues of vesicle-associated membrane protein-associated (VAMP-associated) proteins. Biochem. Biophys. Res. Commun. 254, 0–26. https://doi.org/10.1006/bbrc.1998.9876.

Ohnesorge, S., Bejarano, E.R., 2010. Begomovirus coat protein interacts with a small heat-shock protein of its transmission vector (*Bemisia tabaci*). Insect Mol. Biol. 18, 693–703. https://doi.org/10.1111/j.1365-2583.2009.00906.x.

Pan, L.L., Chen, Q.F., Zhao, J.J., Guo, T., Wang, X.W., Hariton-Shalev, A., Czosnek, H., Liu, S.S., 2017. Clathrin-mediated endocytosis is involved in *Tomato yellow leaf curl virus* transport across the midgut barrier of its whitefly vector. Virology 502, 152–159. https://doi.org/10.1016/j.virol.2016.12.029.

Rana, V.S., Popli, S., Saurav, G.K., Raina, H.S., Chaubey, R., Ramamurthy, V.V., Rajagopal, R., 2015. A *Bemisia tabaci* midgut protein interacts with begomoviruses and plays a role in virus transmission. Cell Microbiol. 18, 663–678. https://doi.org/10.1111/cmi.12538.

Rana, V.S., Popli, S., Saurav, G.K., Raina, H.S., Jamwal, R., Chaubey, R., Ramamurthy, V.V., Natarajan, K., Rajagopal, R., 2019. Implication of the whitefly, *Bemisia tabaci*, collagen protein in begomoviruses acquisition and transmission. Phytopathology (in press). Available at: doi: https://doi.org/10.1094/PHYTO-03-18-0082-R.

Rana, V.S., Sing, S.T., Priya, N.G., Kumar, J., Rajagopal, R., 2012. *Arsenophonus* GroEL interacts with CLCuV and is localized in midgut and salivary gland of whitefly *B. tabaci*. PLoS One 7, e42168. https://doi.org/10.1371/journal.pone.0042168.

Roof, D.J., Hayes, A., Adamian, M., Chishti, A.H., Li, T., 1997. Molecular characterization of abLIM, a novel actin-binding and double zinc finger protein. J. Cell Biol. 138, 575–588. https://doi.org/10.1083/jcb.138.3.575.

Rosen, R., Kanakala, S., Kliot, A., Pakkianathan, B.C., Farich, B.C., Santana-Magal, N., Elimelech, M., Kontsedalov, S., Lebedev, G., Cilia, M., Ghanim, M., 2015. Persistent, circulative transmission of begomoviruses by whitefly vectors. Curr. Opin. Virol. 15, 1–8. https://doi.org/10.1016/j.coviro.2015.06.008.

Sadler, I., Crawford, A.W., Michelsen, J.W., Beckerle, M.C., 1992. Zyxin and cCRP: two interactive LIM domain proteins associated with the cytoskeleton. J. Cell Biol. 119, 1573–1587. https://doi.org/10.1083/jcb.119.6.1573.

Saurav, G.K., Rana, V.S., Popli, S., Daimei, G., Rajagopal, R., 2019. A thioredoxin-like protein of *Bemisia tabaci* interacts with coat protein of begomoviruses. Virus Genes 55, 356–367. https://doi.org/10.1007/s11262-019-01657-z.

Schmeichel, K.L., Beckerle, M.C., 1994. The LIM domain is a modular protein-binding interface. Cell 79, 211–219. https://doi.org/10.1016/0092-8674(94)90191-0.

Scholthof, K.B.G., Adkins, S., Czosnek, H., Palukaitis, P., Jacquot, E., Hohn, T., Hohn, B., Saunders, K., Candresse, T., Ahlquist, P., Hemenway, C., Foster, G., 2011. Top 10 plant viruses in molecular plant pathology. Mol. Plant Pathol. 12, 938–954. https://doi.org/10.1111/j.1364-3703.2011.00752.x.

Skehel, P.A., Fabian-Fine, R., Kandel, E.R., 2000. Mouse VAP33 is associated with the endoplasmic reticulum and microtubules. Proc. Natl. Acad. Sci. U.S.A. 97, 1101–1106. https://doi.org/10.1073/pnas.97.3.1101.

Tsunoda, S., Sierralta, J., Sun, Y., Bodner, R., Suzuki, E., Becker, A., Socolich, M., Zuker, C.S., 1997. A multivalent PDZ-domain protein assembles signalling complexes in a G-protein-coupled cascade. Nature 388, 243–249. https://doi.org/10.1038/40805.

Turner, C.E., Miller, J.T., 1994. Primary sequence of paxillin contains putative SH2 and SH3 domain binding motifs and multiple LIM domains: identification of a vinculin and pp125Fak-binding region. J. Cell Sci. 107, 1583–1591. https://doi.org/10.1083/jcb.125.6.1417.

Uchibori, M., Hirata, A., Suzuki, M., Ugaki, M., 2013. *Tomato yellow leaf curl virus* accumulates in vesicle-like structures in descending and ascending midgut epithelial cells of the vector whitefly, *Bemisia tabaci*, but not in those of nonvector whitefly *Trialeurodes vaporariorum*. J. Gen. Plant Pathol. 79, 115–122. https://doi.org/10.1007/s10327-012-0426-2.

Wang, Z.Z., Shi, M., Huang, Y.C., Wang, X.W., Stanley, D., Chen, X.X., 2016. A peptidoglycan recognition protein acts in whitefly (*Bemisia tabaci*) immunity and involves in begomovirus acquisition. Sci. Rep. 6, 37806. https://doi.org/10.1038/srep37806.

Weir, M.L., Klip, A., Trimble, W.S., 1998. Identification of a human homologue of the vesicle-associated membrane protein (vamp)-associated protein of 33kda (vap-33): a broadly expressed protein that binds to vamp. Biochem. J. 333, 247–251. https://doi.org/10.1042/bj3330247.

Xia, H., Winokur, S.T., Kuo, W.L., Altherr, M.R., Bredt, D.S., 1997. Actinin-associated LIM protein: identification of a domain interaction between PDZ and spectrin-like repeat motifs. J. Cell Biol. 139, 507–515. https://doi.org/10.1083/jcb.139.2.507.

Xia, W.Q., Liang, Y., Chi, Y., Pan, L.L., Zhao, J., Liu, S.S., Wang, X.W., 2018. Intracellular trafficking of begomoviruses in the midgut cells of their insect vector. PLoS Pathog. 14, e1006866. https://doi.org/10.1371/journal.ppat.1006866.